

Interaction of a laser-produced plasma with a solid surface

M. A. Mazing, P. Ya. Pirogovskiy, A. P. Shevelko, and L. P. Presnyakov
P. N. Lebedev Physical Institute, Academy of Sciences of the U.S.S.R., Moscow, U.S.S.R.
 (Received 1 April 1985)

In the present work a solid surface is placed in the propagation path in a laser-produced plasma. A substantial increase in the total emission intensity is observed in the resonance lines of the hydrogenlike and heliumlike ions. The results in the x-ray-wavelength range are given spatially along the propagation path. Dynamics of the plasma-wall interaction process is studied in the visible range with both spatial and temporal resolution.

I. INTRODUCTION

The interaction of a plasma, which contains highly charged ions, with a solid surface is of interest with respect to obtaining intense x-ray line spectra of multiply-charged ions¹ and for many current applications (see, for example, Refs. 2 and 3). Reference 1 showed that there is intense x-ray emission when a burst of hot laser-induced plasma reaches a solid surface. Specifically, the lines of the principal (Lyman) series of hydrogenlike and heliumlike ions are several times more intense than the same lines in the hot core of a laser plasma. In the present paper we give some results concerning emission parameters near the obstacle surface for a magnesium plasma. The x-ray spectra and pinhole plasma images were recorded spatially along the propagation path. In the visible range the results were obtained with both spatial and temporal resolution.

II. EXPERIMENT

The plasma was produced by making use of the second harmonic ($\lambda=0.53 \mu\text{m}$) of a neodymium-glass laser. The energy of the laser pulse could be varied up to 10 J; the pulse duration was 2 ns. The beam was focused by a lens with a focal length of 300 mm onto the plane surface of a magnesium target oriented at 45° from the axis of the incident laser beam (see Fig. 1). The diameter of the focal spot on the target surface was about $30 \mu\text{m}$. The magnesium plasma at the target had an electron temperature of $T_e=500-700 \text{ eV}$ and contained mainly bare nuclei, and hydrogenlike and heliumlike Mg ions. An aluminum plate was placed in the path of the laser burst along the normal to the axis of the burst. The distance between the target and the obstacle along the burst axis was $r_0=1.2-1.5 \text{ mm}$, which was an optimum value for the present measurements. At wider separations, $r \gg r_0$, intensity in the x-ray wavelength range decreases due to decreasing plasma density in the expanding burst. If r is few times less than r_0 , the two regions of intense emission, near the target and near the obstacle, overlap.

The following three techniques were used in the experiments: (i) investigation of temporal-spatial emission parameters in the visible range with the use of a streak cam-

era (see Fig. 1); (ii) recording an image of the plasma burst in the soft x-ray wavelength range, $\lambda \lesssim 10 \text{ \AA}$, using a pinhole camera (see Fig. 3); and (iii) recording an image of the plasma burst in the light of the spectral lines of hydrogenlike and heliumlike magnesium ions ($\lambda=6-10 \text{ \AA}$) using an x-ray crystal Hamos spectrograph⁴ (Fig. 4). All the spectrograms were recorded in a single laser shot.

A. Temporal-spatial parameters of plasma emission in the visible range

A typical time-resolved structure of the burst emission is given in Fig. 1. The results are given in Fig. 2 in the form of spatial-temporal ($r-t$) diagrams for emission of the laser-plasma burst in the target-obstacle region.

From these ($r-t$) diagrams it is possible to derive three pertinent zones which are separated both spatially and temporally. (i) The first is a zone in the immediate vicinity of the magnesium target; this zone corresponds to the free unperturbed expansion of the laser burst [Fig. 2(a)]. (ii) The second zone is located near the obstacle where the burst reaches the aluminum surface; this is the interaction zone [Fig. 2(a)]. (iii) The third is a recoil zone which is

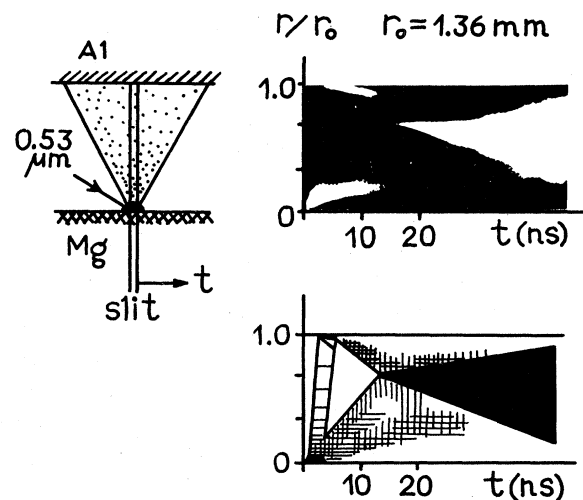


FIG. 1. Space-temporal structure of visible plasma emission (at the top) and the corresponding ($r-t$) diagram (below).

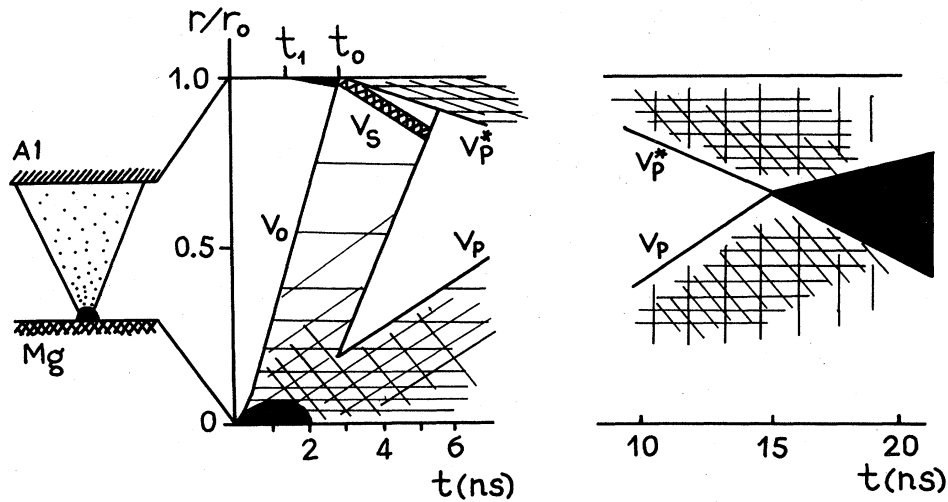


FIG. 2. (a) (r - t) diagram of the visible burst emission in the immediate vicinity of the magnesium target (zone I—the free unperturbed expansion of the laser burst) and in the plasma-wall interaction zone (zone II). (b) (r - t) diagram of the emission in a recoil zone (zone III).

formed at a later stage after plasma expansion from the obstacle surface [Fig. 2(b)].

The results of observations can be summarized as follows.

(1) The asymptotic velocity v_0 of the laser-plasma burst expansion is $\approx 5 \times 10^7 \text{ cm s}^{-1}$; at the moment when the laser pulse is switched off the velocity of the plasma front is $v_p \approx 6 \times 10^6 \text{ cm s}^{-1}$.

(2) When the laser-plasma burst interacts with the obstacle surface, intense emission is observed from the immediate vicinity of the surface. This plasma front is moving back with a velocity $v_p \approx 3 \times 10^6 \text{ cm s}^{-1}$. Intense emission is observed also from a shock-wave front which propagates from the surface with $v_s \approx 1 \times 10^7 \text{ cm s}^{-1}$.

(3) Long-lived intense emission is observed coming from the recoil zone, where the plasma flux expanding from the target after completion of the laser pulse collides with the plasma flux from the obstacle surface.

(4) Some emission from the obstacle-surface region appears at $t=t_1$ even before the moment $t=t_0$ when the burst front reaches the surface [see Fig. 2(a)]. Under the experimental conditions, the target-surface distance $r_0 = 1.36 \text{ mm}$ and the front velocity $v_0 = 5 \times 10^7 \text{ cm s}^{-1}$ give $t_0 = r_0/v_0 \approx 3 \text{ ns}$, whereas $t_1 \approx 1.5 \text{ ns}$. The fact that $t_1 < t_0$ enables us to assume the presence of a small fraction of fast ions in the laser burst with a mean velocity $v = r_0/t_1 \approx 10^8 \text{ cm s}^{-1}$. Emission at $t_1 < t_0$ may arise from either a plasma, which is produced on the surface by fast ions, or recombinative radiation of fast ions.

B. Image of a plasma in soft x-ray range

Our main results are represented in Fig. 3. They were obtained simultaneously with the spatial-temporal structures shown in Figs. 1 and 2, during the same laser shot. An optical density D (solid curve) was measured along the expanding burst path without integration over emission

volumes. The dashed curve represents values of D at distances above 0.5 mm if the obstacle surface is absent. A substantial increase in the x-ray emission intensity was observed in two separate regions. The first is located near the obstacle surface. It is possible to compare a bright

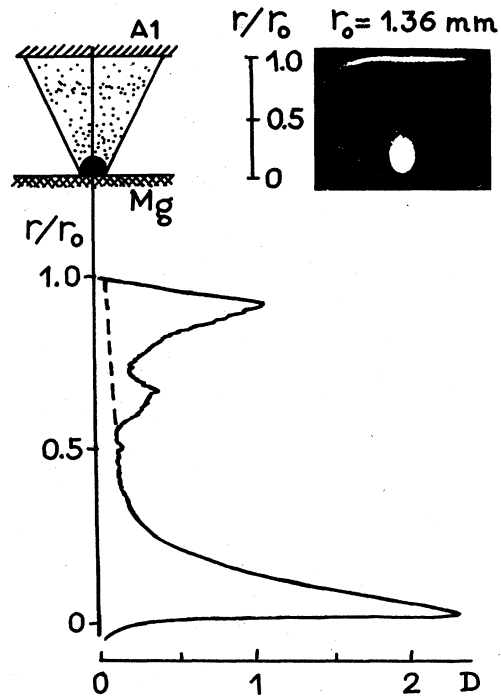


FIG. 3. Microdensitometer tracing of the soft x-ray burst emission ($\lambda \leq 10 \text{ \AA}$) in the laser-plasma-wall interaction zone (D is the optical density). The dashed curve represents values of D at distances above 0.5 mm if the obstacle surface is absent.

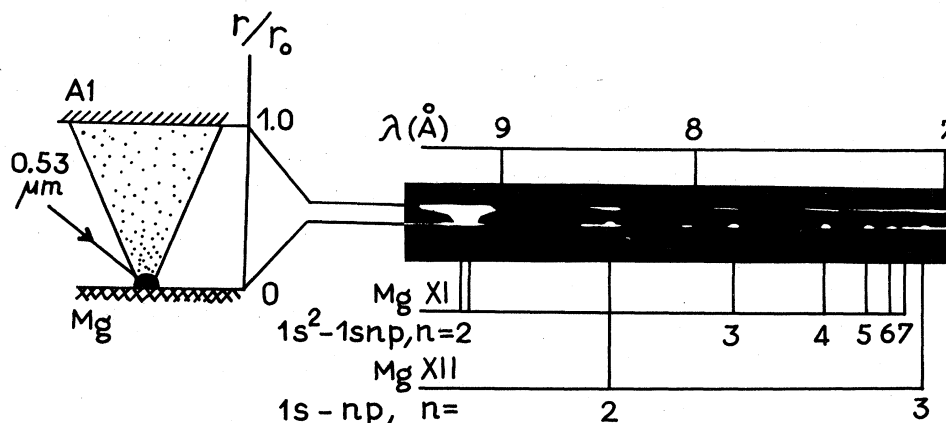


FIG. 4. Image of the plasma in the light of spectral lines of H- and He-like magnesium ions in the plasma-wall interaction.

splash here with structures shown in Fig. 2(a). The second region is less intense and may be connected to the recoil zone shown in Fig. 2(b).

C. Image of a plasma in the light of spectral lines

The Hamos x-ray crystal spectrograph formed a two-dimensional image of the plasma in the light of spectral lines. In this case, a spectral linewidth was defined by the source size d . For the target zone, $d \approx 100 \mu\text{m}$ and the value of spectral resolution, $\lambda/\Delta\lambda$ is equal to 700. For the interaction zone, $d \approx 1 \text{ mm}$ and $\lambda/\Delta\lambda \sim 100$.

When the plasma burst reaches the obstacle surface, intense emission is observed in the lines of the principal series of H- and He-like magnesium ions, whereas all the satellite lines are absent (see Fig. 4). There are two regions of line emission: the hot core of the plasma (up to $100 \mu\text{m}$ from the magnesium target) and the active layer at the obstacle surface; between them there is a region without x-ray spectral lines. The relative intensities of the emission in the pertinent part of the spectrum of the burst and of the surface region are 1.0 and 1.3 for the resonance line of the hydrogenlike ion Mg XII ($\lambda = 8.42 \text{ \AA}$), and they are 1.1 and 3.6 for the resonance line of the heliumlike ion Mg ($\lambda = 9.17 \text{ \AA}$). The resultant intensity of the resonance lines of the Mg XI and Mg XII ions near the surface is thus 2.5 times their intensity on the hot-burst core. This effect does not depend on the surface material: the spectrum does not change when the aluminum is replaced by polyethylene. We should note that in the case of aluminum there are no lines of highly stripped aluminum ions. This result implies that the electrons near the surface are at a low temperature. This electron temperature ($T_e^S = 50 + 100 \text{ eV}$) was obtained from radiative-recombination Mg XII \rightarrow Mg XI spectra, whereas the temperature of the hot-burst core is much larger ($T_e^B \approx 600 \text{ eV}$).

III. DISCUSSION AND CONCLUSIONS

The results above show that the main increase in the total x-ray emission intensity is observed near the obstacle surface where $I/I_0 \geq 10$ (here I_0 is the emission intensity in the burst without the obstacle). The emission in the surface region results from the capture of electrons to

high-lying levels of multiply-charged magnesium ions, followed by cascade transitions due to radiative and collisional processes. The capture may have several reasons: radiative recombination and charge exchange of ions with surface atoms or both processes in a near-surface secondary plasma,¹ or radiative and three-body recombination of ions in a density jump produced by a shock wave.²

A simple shock-wave picture is usually based on the assumption of the "ideal" wall and boundary conditions which do not employ effects of mass and energy penetration through the surface, and of ion accumulation near the surface. However, the ion-accumulation effect may lead to a substantial increase in the total x-ray emission intensity in the immediate vicinity of the obstacle surface. Using the data given in Ref. 3 for magnesium ions, we can estimate a coefficient of reflection R from the aluminum surface. Under our experimental conditions, $R = 10 + 20\%$. It means that most of the magnesium must stop inside the aluminum plate; the mean-free path of a magnesium ion in aluminum is about 300 \AA .⁵

Another important effect is sputtering of the surface material. In our case the gaseous-dynamics flux density of ions is about $3 \times 10^{10} \text{ W cm}^{-2}$, and according to Ref. 3 the sputtering coefficient varies from 1.0 up to 10. Thus, the ion bombardment leads to the production of a secondary plasma layer near the surface. This fact is confirmed by experiments^{1,6} in which the surface material was polyethylene $(\text{CH}_2)_n$ and the ions C II–C VI were observed. Special investigation⁶ showed that ionization of the surface material results from the particles of the laser-plasma burst; x-ray laser-plasma emission and a reflected laser beam are not important.

A detailed quantitative explanation of the intense x-ray emission near a surface requires the analysis of nonstationary transient plasmas simultaneously with many elementary processes of collisional radiative recombination and with the charge exchange of highly charged ions with neutral atoms and low- Z ions in a secondary plasma; the direct capture of electrons from the surface is of interest also.

The present results demonstrate a new and promising way to produce intense x-ray recombination emission through the interaction of a laser plasma with a solid.

- ¹L. P. Presnyakov and A. P. Shevelko, *Pis'ma Zh. Eksp. Teor. Fiz.* **36**, 38 (1982) [*JETP Lett.* **36**, 44 (1982)].
- ²V. A. Boiko, B. A. Bryunetkin, F. V. Bunkin, V. I. Derzhiev, V. M. Dyakin, I. Yu. Skobelev, A. Ya. Faenov, A. I. Fedosimov, K. A. Shilov, S. I. Yakovlenko, *Kvant. Elektron. (Moscow)* **10**, 901 (1983) [*Sov. J. Quantum Electron.* **13**, 565 (1983)]; *Pis'ma Zh. Tekh. Fiz.* **9**, 673 (1983) [*Sov. Tech. Phys. Lett.* **9**, 289 (1983)].
- ³R. Behrish, *Sputtering by Particle Bombardment (Physical Sputtering of Single-Element Solids)* (Springer, New York, 1981).
- ⁴L. Hamos, *Ann. Phys. (Leipzig)* **17**, 716 (1933).
- ⁵J. F. Gibbons, W. S. Johnson, and S. W. Mylroie, *Projected Range Statistics* (Dowden, Hutchinson and Ross, Stroudsburg, Pennsylvania, 1975).
- ⁶N. Yamaguchi and S. Ohtani, *Annual Review, Institute of Plasma Physics, Nagoya, Japan, 1982*, pp. 151–153 (unpublished).